Journal Pre-proofs

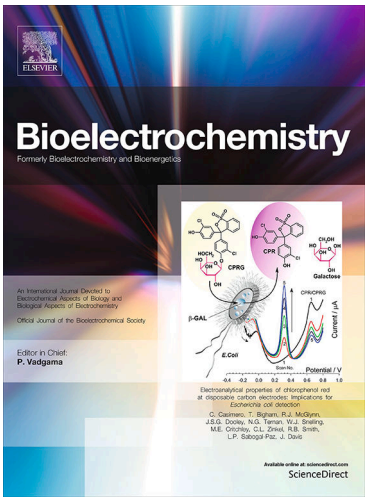

Flow-through laminar anodes with variable interlaminar distance to modulate the current density of urine-fed bio-electrochemical systems

Mariano Prudente, Diego A. Massazza, Raúl A. Procaccini, Nicolás A. Rodríguez, Hernán E. Romeo

PII: S1567-5394(23)00045-2
DOI: https://doi.org/10.1016/j.bioelechem.2023.108408
Reference: BIOJEC 108408

To appear in: *Bioelectrochemistry*

Received Date: 9 January 2023
Revised Date: 24 February 2023
Accepted Date: 24 February 2023

Please cite this article as: M. Prudente, D.A. Massazza, R.A. Procaccini, N.A. Rodríguez, H.E. Romeo, Flow-through laminar anodes with variable interlaminar distance to modulate the current density of urine-fed bio-electrochemical systems, *Bioelectrochemistry* (2023), doi: https://doi.org/10.1016/j.bioelechem.2023.108408

Flow-through laminar anodes with variable interlaminar distance to modulate the current density of urine-fed bio-electrochemical systems

Mariano Prudente,[a,b] Diego A. Massazza,[b] Raúl A. Procaccini,[c] Nicolás A. Rodríguez[d,e] and Hernán E. Romeo [a]*

[a]*Nanostructured Polymers Division*

[b]*Bio-procesess and Interface Engineering Division*

[c]*Applied Electrochemistry Division*

[d]*Ceramics Division*

[a,b,c,d] *Institute of Materials Science and Technology (INTEMA), National Research Council (CONICET), Mar del Plata, Argentina.*

[e]*Department of Chemistry and Biochemistry, School of Exact and Natural Sciences, University of Mar del Plata (UNMdP), Mar del Plata, Argentina.*

Corresponding author:* ***hromeo@fi.mdp.edu.ar*

Abstract

Three-dimensional (3D) porous anodes used in urine-powered bio-electrochemical applications usually lead to the growth of electro-active bacteria on the outer electrode surface, due to limited microbial access to the internal structure and lack of permeation of culture medium through the entire porous architecture. In this study, we propose the use of 3D monolithic Ti_4O_7 porous electrodes with controlled laminar structures as microbial anodes for urine-fed bio-electrochemical systems. The interlaminar distance was tuned to modulate the anode surface areas and, thus, the volumetric current densities. To profit from the true area of the electrodes, urine feeding was performed as a continuous flow through the laminar architectures. The system was optimized according to the response surface methodology (RSM). The electrode interlaminar distance and the concentration of urine were selected as independent variables, with the volumetric current density as the output response to optimize. Maximum current densities of 5.2 $kA.m^{-3}$ were produced from electrodes with 12 μm-interlaminar distance and 10 %v/v urine concentrations. The present study demonstrates the existence of a trade-off between the accesibility to the internal electrode structure and the effective usage of the surface area to maximize the volumetric current density when diluted urine is used as flowing-through feeding fuel.

Keywords: bio-electrochemical systems; urine; porous anodes; response surface methodology.

1. Introduction

Microbial fuel cells (MFCs) are electrochemical devices that make use of the metabolic machinery of electro-active bacteria to turn organic matter into electricity [1-3]. The use of human urine as a source of organic matter to feed the anodic compartment of MFCs is a common practice nowadays [4-6]. Ongoing efforts are being made to improve the energy recovery efficiency of urine-powered MFCs, covering a variety of aspects such as reactor type [7], cell configuration, feeding modes and residence times [8]; as well as variables related to the acclimation of the electro-active microorganisms to increasing urine concentrations [9] and/or management of the urine concentration itself as a strategy to increase the electrical charge recovered [10].

Out of the variables involved in the charge recovery phenomenon, the interaction between the anode material and the electro-active microorganisms (so as to enhance both microbial adhesion and the electron transfer efficiency) has been particularly addressed in the last years in the field of bio-electrochemistry [11]. This interaction, along with the mass transport phenomena associated to the flow of substrate to the biofilm surface (advection and diffusion), ultimately controls the microbial metabolic activity [12], which is responsible for the final conversion of organic matter into electricity. In this scenario, the pursuit of increasingly efficient bacteria/anode interfaces has led to the use of three-dimensional (3D) porous anodes, as a direct way of increasing the contact surface area between the microorganisms and the current colector [13-15]. The main goal has been to boost the anodic volumetric current density (current per anode unit volume), which requires the simultaneous increase of the electrochemically-active area per unit volume and the electrical current per unit area, the latter depending on the electrode microbial colonization [16]. A simple analysis shows that, for a fixed anode porosity, both requirements are not possible to simultaneously meet, as a consequence of the inverse relationship between the volumetric surface area and pore size, the latter directly determining the ease of microbial penetration inside the electrode. Accordingly,

the optimization of the microbial anode architecture falls into a compromise. The efforts made to date have been mainly headed to increase simultaneously the porosity of the electrodes and the pore size, to promote microbial colonization deep inside the electrode structure. The pursuit of an optimum range of pore sizes has revealed that open and connected macropores of the order of 500 μm upwards (up to a few millimeters) appear to represent the best option when internal colonization is the final goal [17], even at the expense of decreasing the effective area. These conclusions have been drawn by evaluating the effect of the pore size on the anodic current densities; however, the latter have been generally calculated on the basis of the projected anode unit area (not true area), which makes the comparison difficult and, in a sense, the conclusions arrived to not entirely valid [18]. Likewise, the optimization of the electrode structure has been also based on the search for conditions that allow for the development of increasingly thicker biofilms inside the electrodes - avoiding simultaneously clogging events - under the inherent assumption that the electrical current recovered scales with biofilm thickness. However, the latter is not completely so when thick biofilms are grown. The occurrence of metabolic constraints in microorganisms associated to electrode interfaces is a well-known phenomenon. Beyond a certain thickness (~ 30-50 μm) electro-active biofilms experience physiological stratification, i.e. the ocurrence of redox gradients along the biofilm matrix, leading to the progressive accumulation of microbial cells that do not contribute to current production [19,20]. As a consequence, it is only within the mentioned order of magnitude of biofilm thickness that current scales linearly with microbial biomass [21,22], departing from the optimum metabolic performance when growing beyond that limit. In this context, it would not be necessary to reach millimiter-sized pores to allow for thicker biofilms to grow to optimize the performance of 3D porous microbial anodes. Indeed, the analysis of the literature reveals that, when electro-active microorganisms have access to large surface areas and are not limited in substrate, the formation of thin films (of the order of 10-20 μm thickness) is the preferred event, even in the presence of pores of hundred of microns, which would

theroretically allow the growth of thicker microbial conglomerates [13,23,24]. We demonstrated this effect in model bio-electrochemical systems, by using 3D porous laminar anodes with interlaminar distances in the order of tens of microns [25].

In the context of urine-fed bio-electrochemical systems, the configurations so far addressed have used, in most cases, two-dimensional (2D) anodes, such as graphite plates, carbon fiber veils [26,27], carbon cloth [28] and graphite felts [29]. While the latter have been usually considered as 3D porous platforms, their woven fiber geometry (closed and intricate) leads mainly to the growth of electro-active biofilms on the outer surface of the electrode, in a way such that its performance finally resembles that of typical 2D anodes. Furthermore, the porous anodes addressed to date have not been used under a continuous flow of urine through their porous architectures [30], which is clearly detrimental when profiting from a large surface area per unit volume is the main goal.

In the present study, we propose the use of 3D monolithic Ti_4O_7 porous electrodes with controlled laminar architectures as microbial anodes for urine-powered bio-electrochemical applications. The interlaminar distance of the electrodes was tuned in the range of tens of microns to modulate the anode surface area per unit volume and, thus, the volumetric current densities. To profit from the true area of the electrodes, urine feeding was performed under a continuous flow through the laminar structures. Instead of searching for the optimization of the microbial anodes through the analysis of one experimental variable at a time, a multivariate approach - according to the response surface methodology (RSM) - was introduced. The electrode layer-to-layer distance and the concentration of urine were selected as the independent variables, with the anodic volumetric current density as the dependent variable to optimize. The optimization of the anode performance through an statistical approach granted the prediction of pairs of experimental variables that together maximized the current per anode unit volume. The maximum current density obtained in the present study turned out to be one order of magnitud higher than those so far reported for 3D porous anodes in the context of urine-fed bio-

electrochemical systems, which might represent a valuable boost towards the consolidation of sustainable bio-electrochemical devices ran on human urine. The present study demonstrates the existence of a trade-off between the accesibility to the internal electrode structure (controlled by the interlaminar distance) and the effective usage of the anode surface area to maximize the volumetric current density when diluted urine is used as feeding fuel under a flow-through regime.

2. Materials and methods

2.1. Preparation of laminar electrodes

Porous Ti_4O_7 electrodes with laminar architecture were prepared *via* directional freezing of TiO_2 aqueous dispersions, followed by sintering and chemical reduction at high temperature.

To prepare the aqueous dispersions, 0.93 g of poly(vinylpirrolidone) (PVP, 1.3 MDa, Aldrich) were first dissolved in 15 mL of Milli-Q water (without stirring, to avoid the formation of bubbles), to which 3.15 g of TiO_2 nanoparticles (P25, Degussa) were finally added (under gentle stirring). Homogeneous dispersions were obtained by mechanical stirring for another 30 min. The dispersions were then poured into plastic moulds (cylinders of 8 cm length and 1.3 cm diameter) and immersed into a cold bath at a controlled constant rate according to reported protocols of our group [14,25], inducing the oriented growth of laminar ice crystals in the dispersions. The thickness of the ice crystals was tuned by controlling both the immersion rate (1 or 3 $mm.min^{-1}$) and/or the temperature of the cold bath (-196ºC, -70ºC or -30ºC). Once frozen, the samples were freeze-dried for 48 h (100 mTorr) to remove the ice and create the laminar-like porosity. The TiO_2 porous monoliths obtained after the freeze-drying process were cut into pieces (2.5 cm length) and were subjected to a sintering protocol in an air atmosphere (1.5 h at 1000°C, heating and cooling rates of $5°C.min^{-1}$) to obtain mechanically stable porous platforms. The total open porosity of the monolithic pieces was kept constant ($\varepsilon \sim 88$-90%) (see Section 2.4), which was controlled with the amount of water in the initial dispersions.

According to the experimental conditions used, self-standing porous structures with interlaminar distances spanning 5 to 27 μm were obtained (Section A, Supporting Information).

Electrically conducting Ti_4O_7 monoliths were obtained from the sintered structures, after a reducing protocol with elemental Zr (15 mg Zr/100 mg TiO_2) at high temperature (1000°C) under vacuum, according to reported procedures [31]. The conducting laminar platforms were finally used as urine-fed flow-through electrodes to grow electro-active microorganisms inside their structures.

For comparative purposes, a non-porous Ti_4O_7 electrode was used as a control. The non-porous electrode was prepared from the same TiO_2 dispersion used for obtaining the porous platforms, but in this case the dispersion was first dried (50ºC) to obtain a powder that was subsequently pressed at 2.8 $Tn.cm^{-2}$ to produce cylinders of 1.3 cm length and 1 cm diameter. Thus-prepared TiO_2 cylinders were finally sintered (1.5 h at 1000ºC). After sintering, the dimmensions of the pieces were 1.1 cm (length) and 0.9 cm (diameter). Sintered samples were finally heat-treated in the presence of metallic Zr (same experimental procedure described for the porous electrodes) to obtain the electrically conducting phase, Ti_4O_7.

2.2. Microbial inoculum source and urine samples

A sludge collected from the wastewater treatment plant at the Institute of Materials Science and Technology (INTEMA, Mar del Plata, Argentina) was used as the microbial inoculum source. According to previous studies [10], to enrich the inoculum in a broad mixed anaerobic consortium, graphite bars (8.05 cm^2 exposed area) were initially set into an anaerobic reactor (three-electrode bio-electrochemical cell, 160 mL capacity with 10 mL headspace) containing the sludge, and were externally polarized at 0.2 V *vs* Ag/AgCl reference electrode under stirring at 30 °C. To prevent microbial cells from coming into contact with oxygen, the reactor was continuously flushed with a CO_2/N_2 (80/20) gas mixture. The colonization of graphite bars was performed by using a synthetic domestic wastewater (so-called Syntho) as the initial source of

organic matter [32]. After stable current production (one week), colonized bars were removed from the reactors and used as microbial source of sludge-free reactors, which were ultimately used to evaluate the laminar Ti_4O_7 electrodes under a flow-through configuration (see Section 2.3).

The human urine used as feeding fuel was collected from six (6) volunteers after informed consent, according to protocols approved by the Ethics Committee of the University of Mar del Plata (PTIB, UNMdP, Mar del Plata, Argentina). The volunteers were selected according to their age, body size and diet, in order to address urine variability depending on those physiological conditions, counting on a representative sampling case. The collected urine was pooled together and used the day of collection without any pre-treatment [10].

2.3. Electro-analysis cell and bio-electrochemical assays

When the characterization of microbial anodes is the main objective under research, three-electrode configurations represent the optimum design for exploring the intrinsic anode behaviour [33]. This ensures that the bio-anode is the sole rate-limiting step in the current generation process, at the time that the potential of the anode is perfectly controlled, not being affected by the kinetics of the cathode or any other variation of the system [33,34]. In line with this, and according to the goal of the present study, potentiostat-controlled three-electrode set-ups were used as experimental reactors (160 mL capacity, 10 mL headspace).

The prepared laminar Ti_4O_7 structures were used as the working electrodes. For this, they were separately set in different three-electrode cells and poised at a constant potential of 0.2 V *vs* Ag/AgCl reference electrode, using platinum coils as counter-electrodes. Axially-hollowed graphite bars were used to make the electrical contact to the external circuit, gluing them on the working electrodes by using a conducting adhesive, according to previous studies [14,25]. Graphite contacts were prevented from touching the liquid culture medium. To evaluate the effect of the interlaminar distance on the output performance, fresh culture medium was

continuously passed through the laminar anodes, by making use of the hollowed conduct along the graphite bars, containing a rubber hose in it. A peristaltic pump was employed to deliver the culture medium at a flow rate of 3 $mL.h^{-1}$. This flow rate was selected according to preliminary studies, after evaluating the current output as a function of urine flow. The flow-through experimental set-up is shown in the Section B of the Supporting Information. The reactors and all liquid reservoirs were kept at 30 °C, while continuously flushed with a gas mixture (CO_2/N_2, 80/20) to prevent them from oxygen contamination. The inoculation of each cell was naturally achieved by crossed-colonization, from the colonized graphite bars coming from the inoculum reactor (Section 2.2). To allow for the initial bacterial growth and proliferation of microorganisms inside the polarized porous electrodes, the reactors were first left in batch mode for 5 days, after which they were turned into a continuous flow-through mode along the laminated structures. In the case of the non-porous control electrode, and faced the impossibility of performing a flow-through feeding mode, a ´lateral port´ on the reactor lid (slightly displaced from the central port used to set the electrode) was used to flow the urine medium directly into the reactor.

In all cases the initial culture medium consisted of synthetic wastewater (Syntho), being progressively changed (every 10 days) to a different medium composition prepared from mixtures of Syntho and human urine to span urine concentrations from 0 to 15 %v/v, according to an acclimation protocol developed for this purpose [10]. The physical-chemical properties (pH and ionic conductivity) and composition (urea content, ammonium concentration and total organic concentration, the latter given as chemical oxygen demand, COD) of each feeding medium are summarized in the Section B (Supporting Information). The production of current was followed in time by chronoamperometry. Current densities were calculated based on both the anode volume and the true electrode area (not projected). The results shown represent the mean of two independent tests for each electrode.

2.4. Characterization

Laminar features of the electrode structures were assessed by scanning electron microscopy (SEM), by using a FEI (Quanta 200) instrument. Prior to the observations, samples were covered with a thin gold layer.

Bulk (apparent) densities of the electrodes were calculated from the weight and volume of each specimen. The porosity of the electrodes (ε%) was determined from:

$$\varepsilon\% = \left(1 - \frac{\delta c}{\delta r}\right) \text{ x } 100 \qquad (1)$$

where δ_c corresponds to the calculated bulk densities and δ_r to the reported skeletal density for Ti_4O_7 (4.32 $g.cm^{-3}$) [31].

Cyclic voltammetry (CV) analyses of the microbial anodes were performed using a VoltaLab10 PGZ-100 (Radiometer Analytical) potentiostat/galvanostat, by scanning a potential range between - 0.5 V and 0.5 V at a rate of 0.01 $V.s^{-1}$.

Surface areas per electrode unit volume were calculated from double-layer capacitance values (C_{dl}, apparent capacitance), obtained by CV according to reported protocols [35,36]. CV analyses were conducted in a three-electrode reactor by using a VoltaLab10 PGZ-100 (Radiometer Analytical) potentiostat/galvanostat. A 0.1 M Na_2SO_4 solution was used as a supporting electrolyte, a saturated Calomel electrode (SCE) was the reference, a platinunm coil was set as the counter-electrode and the laminated Ti_4O_7 structures were used as the working electrodes (separately tested). Different scan rates (0.002, 0.003, 0.004, 0.005, 0.006 $V.s^{-1}$) were used over a potential window of -0.35 V / 0.35 V *vs* SCE. The values of C_{dl} were determined by linear regression of current (A) *vs.* scan rate (V/s) curves. The electro-active areas were calculated by dividing the C_{dl} values obtained for each electrode by the effective capacitance (C_{eff}) corresponding to Ti_4O_7. In most of the studies dealing with Ti_4O_7 electrodes a standard capacitance of 60 $\mu F.cm^{-2}$ - corresponding to generic metal oxide surfaces - is usually taken as a representative value for the C_{eff} of the titanium oxide surface. However, this value is not

necessarily applicable to all oxides regardless of the nature of the metal ion involved and/or the hydration degree of its surface. Accordingly, we first calculated the C_{eff} corresponding strictly to the Ti_4O_7 material under the experimental conditions used. For this, electrochemical impedance spectroscopy (EIS) was used (Gamry Ref600 instrument) under AC modulation between 100000 and 0.01 Hz. Three-electrode cells were employed for the measurements, with 0.1 M Na_2SO_4 solution as the supporting electrolyte, a saturated Calomel electrode (SCE) as the reference and a platinum coil as the counter-electrode. To simplify the analysis, the non-porous Ti_4O_7 monolith, with an exposed surface area of 0.64 cm^2, was used as the working electrode. Experimental impedance curves were fitted with an equivalent circuit (EC) model developed by using the ZView 3.4e and ZSimpWin 3.21 softwares [37,38]. Details of calculations of C_{eff} and volumetric surface areas for each porous electrode are described in the Supporting Information (Section C).

2.5. Optimization of the bio-electrochemical response

The bio-electrochemical response was optimized by studying the operational conditions of the microbial anodes in the context of the response surface methodology (RSM) [39,40]. Accordingly, instead of testing one experimental variable at a time to evaluate its effect on the response of interest (volumetric current density, *j*), the optimization of the microbial anode performance was approached by simultaneously adressing the change of two experimental parameters. This multivariate approach requieres the initial selection of those parameters known to influence the target variable (*j*), with the objective of making statistical predictions of the behaviour of the system [41].

In a previous work we showed how the immersion rate and temperature of the cold source used in the directional freezing process impacted on the interlaminar distance ($d_{//}$) of porous Ti_4O_7 microbial anodes [25], and how $d_{//}$ in turn conditioned the maximum volumetric current density reached. Likewise, and in the context of a microbial acclimation protocol, we have

demonstrated the effect of the urine concentration ([*urine*]) on the composition of the bacterial community responsible for the current generation in a bio-electrochemical reactor [10]. Accordingly, $d_{//}$ and [*urine*] were considered in this study as the screening parameters to optimize *j*, whose levels (that is, the different values the variable takes in each experiment) are detailed in the Supporting Information (Section D), along with the *j* values experimentally determined for each condition. The current density values obtained (Tables D-1 and D-2 in the Supporting Information) were then fitted with a quadratic model with a two-way interaction, using the RSM library in R [42], according to the following expression:

$$j = x_0 + x_1.\overline{d_{//}} + x_2.\overline{[urine]} + x_{12}.\overline{d_{//}}.\overline{[urine]} + x_{11}.(\overline{d_{//}})^2 + x_{22}.(\overline{[urine]})^2 \qquad (2)$$

where the values of $\overline{d_{//}}$ and $\overline{[urine]}$ correspond to those codified to a dimensionless scale in proportion to their location in the experimental space, as typically done in RSM [41]. This ensures that the coded independent variables change from 1 to -1 in the dimensionless scale, making valid the comparison among the polynomial coefficients (x_i in the Equation (2)) since they all have the same units ($kA.m^{-3}$ in the present study); while simultaneously enabling the processing of variables of different orders of magnitude. For the transformation of the experimental values into the coded values, the following expression was used:

$$\overline{z}_i = \left(\frac{z_i - z_{i,min} - z_{i,hw}}{z_{i,hw}}\right) \qquad (3)$$

where z_i accounts for each of the experimental $d_{//}$ or [*urine*] values (according to the case), $z_{i,min}$ is the minimum experimental value tested for each variable and $z_{i,hw}$ is the half-width value, i. e. $\frac{(z_{i,max} - z_{i,min})}{2}$, with $z_{i,max}$ representing the maximum experimental value tested for the variable under study. Accordingly, $\overline{z}_i$ represents the coded variable ($-1 \leq \overline{z}_i \leq 1$).

The fitting process with the Equation (2) defined a response surface that was finally used for the statistical prediction of $\overline{d_{//}}$ and $\overline{[urine]}$ that together maximize *j* under the experimental conditions used. Coded $\overline{d_{//}}$ and $\overline{[urine]}$ obtained from the fitting process were finally

transformed back to real values ($d_{//}$ and [*urine*]) by using the Equation (3), as indicated by the RSM library. Visual representations of the response surfaces were made with the Plotly library in R by using the real variables. The R file containing the data treatment is publicly available as a complement to the Supporting Information.

3. Results and discussion

3.1. Current density surfaces and bio-electrochemical optimization

Fig. 1(a) shows the volumetric current density surface obtained by evaluating combinations of different urine concentrations ([*urine*] = 0, 5, 10 and 15 %v/v) with anodes of distinct interlaminar distances ($d_{//}$ = 5, 10, 19 and 27 μm), according to the matrix shown in the Supporting Information (Section D, Table D-1). **Fig. 1(b)** depicts a plot of the experimental current densities and their corresponding predicted values according to the fitted multivariate function. A summary of the fitting parameters of this function (x_i elements in the Equation (2)) can be found in the Supporting Information (Section E).

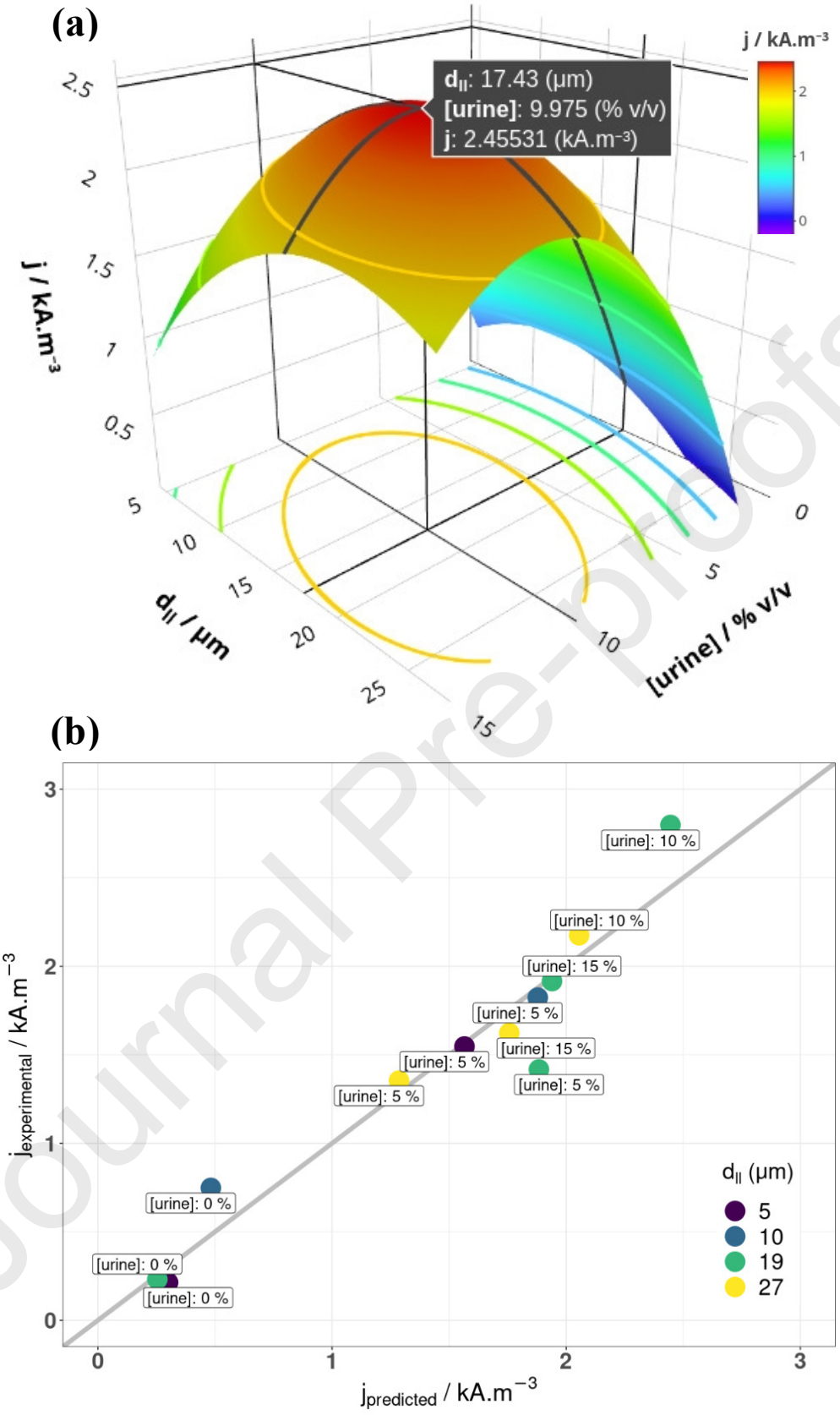

Fig. 1. (a) Response surface obtained by fitting the experimental *j* values with the Equation (2). The coordinates of the maximum are indicated. **(b)** Experimental current densities (symbols) as a function of the predicted values. Coloured symbols identify electrodes with different interlaminar distances.

Regarding the first set of experiments conducted, some details should be mentioned. A few experiments (the ones with electrodes with $d_{//}$ values of 5 or 10 μm) could not be performed over the full range of urine compositions, due to precipitation events at the highest concentrations that led to the clogging of the reactor inlet piping system, reducing the continuous flow through the anode architectures. This led to departures from the experimental conditions set for all of the reactors, making comparisons no longer valid. In a previous study, conducted with non-porous graphite microbial anodes, we discussed the effects caused by the precipitation of inorganic salts in the reactor [10], and the negative consequences of this phenomenon on the output current density when urine concentrations above 20 %v/v were used. In the present work, urine concentrations higher than 10 % seem to have produced inorganic particles large enough to obturate the system piping and the shortest $d_{//}$ values tested. Accordingly, the experimental points corresponding to the mentioned conditions were discarded and not considered for the fitting process (this is indicated in red in the Table D-1, Section D, Supporting Information).

The response surface obtained (**Fig. 1(a)**) was used for optimizing the independent variables tested. This is typically done by ´moving´ on the surface towards - or away from - the critical point, depending on the response of interest and the nature of the critical point. For the case of quadratic models, as the one used in this study, the stationary critical point may represent a maximum, a minimum or a saddle inflection. In the present case the fitting process led to a parabolic-shaped current density surface characterized by a maximum located at [*urine*] ~ 10 %v/v and values of $d_{//}$ ~ 17 μm, the latter being a level not explored in the first set of experiments. The identification of the coordinates of the maximum within the boundaries explored indicates that a substantial modification of the experimental design is not necessary to reach the optimal conditions. In this context it is to be mentioned that, according to the RSM theory, the maximum defines a region in the experimental domain that just serves as a guiding

tool around which it is possible to find the levels of the variables that would optimize the response of interest.

Thus, according to the region predicted around the maximum, a second experimental run was performed, testing microbial anodes with $d_{//}$ values between 10 and 19 µm and [*urine*] around 10 %v/v (Section D, Table D-2, Supporting Information). **Fig. 2** shows the obtained volumetric current density surface. The fitting parameters for this surface can be found in the supplementary R file.

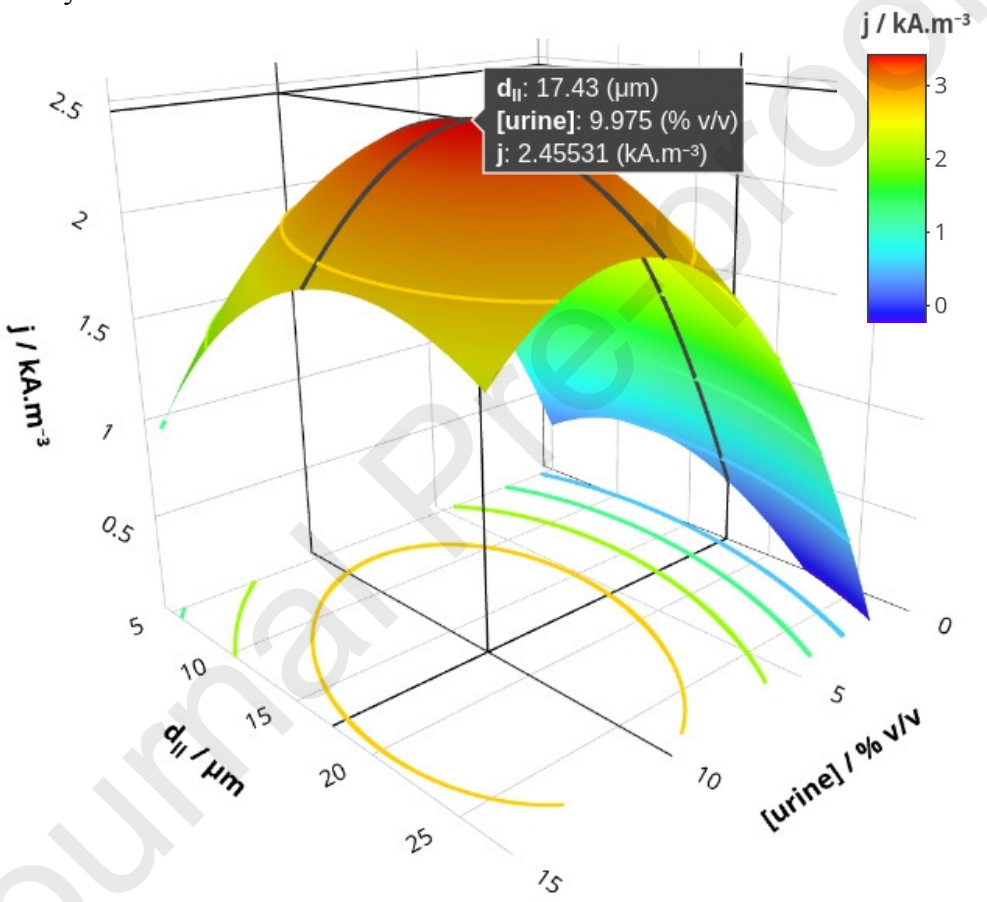

Fig. 2. Response surface corresponding to the second experimental run.

By modifying the interlaminar distance of the electrodes, a substancial increase in the volumetric current densities was achieved. In this context, and considering that each experiment takes over a month to be completed, the RSM approach allowed saving both experimental time and efforts to prepare a number of electrodes to reach the optimal conditions, paving the way to the identification of the levels needed to improve the microbial anode performance.

According to the results of the second experimental run, current densities over 3.5 $kA.m^{-3}$ were obtained with electrodes with $d_{//}$ = 12 µm and [*urine*] in the range 10-15 %v/v (Section D, Table D-2, Supporting Information). Particularly, the electrode E-703 ($d_{//}$ = 12 µm), acclimated up to 10 %v/v urine, led to volumetric densities of 5.21 $kA.m^{-3}$, equating to areal current densities of 3.72 $A.m^{-2}$ (on the basis of the true electrode surface, according to the area determined by cyclic voltammetry; Section C, Table C-2). Compared to previously reported studies under model conditions [25], the $d_{//}$ values that optimized the response under the experimental conditions used in the present work turned out to be shorter than those formerly found. This might be associated to the different flowing conditions employed (36 $mL.h^{-1}$ in ref. [25] for a typical *Geobacter* culture medium, and 3 $mL.h^{-1}$ in the present study for unpretreated human urine), which are known to exert a strong influence on the hydrodynamic boundary layer (HBL) associated to the flow pattern over the biofilm surface; shaping the biofilm structure, the mass transfer phenomena and, accordingly, the microbial developmental stage [12]. This effect has been discussed in the ref. [25], and may have led to changes in the optimum $d_{//}$ values for each experimental condition. By analyzing the second response surface (**Fig. 2**), it can be seen that the coordinates of the maximum only moved slightly on the $d_{//}$ *vs* [*urine*] plane compared to those obtained from the first surface. This indicated that a fine tuning of the levels of the experimental variables might still be addressed for continuing optimizing the anode performance. However, at this level of precision, the inherent experimental error associated to the current density measurements was greater than the fine variations required by the optimization procedure. Accordingly, this fact was taken as a criterion to end up the optimization process under the experimental conditions used.

3.2. Assessment of the surface area usage efficiency

To further assess whether the 3D anodes were taking advantage of their internal surface, a performance factor for the production of current for all of the laminated electrodes was

estimated. For this, the maximum areal current density obtained for the non-porous control electrode (4.2 $A.m^{-2}$) was scaled according to the real surface area of each laminated anode (Section C, Table C-2, Supporting Information), comparing finally the experimental maximum volumetric current densities with the calculated scaled values. In this context, the laminated anodes were considered as an extension of surface per unit volume compared to the non-porous electrode. While this might not be extrictly so - due to different operating processes on the exposed surface of the non-porous anode compared to those ocurring on the confined surface of the laminated architectures - the visualization of the system in this way did indeed allow an internal comparison among the tested electrodes (**Fig. 3**).

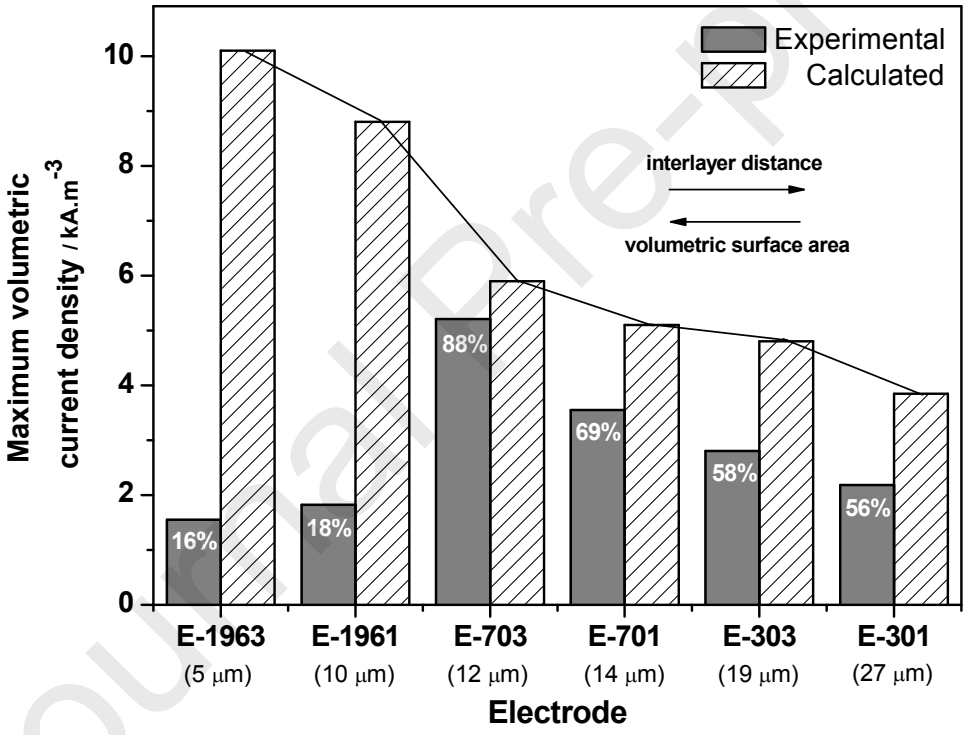

Fig. 3. Electrode performance. Patterned-bars represent the maximum volumetric current densities calculated by scaling the surface current density of the non-porous control Ti_4O_7 electrode (4.2 $A.m^{-2}$) to each laminated electrode according to their true volumetric surface area. Plain-bars represent the maximum experimental volumetric current densities obtained. The performance of the electrodes was estimated as a percentage value respect to the maximum current density attainable assuming total usage of the laminated electrode area $\left(\frac{j_{\max \exp}}{j_{\max calc}} \text{ x } 100\right)$. The mean interlaminar distance (indicated below the electrode nomenclature) increases from E-1963 to E-301, whereas the area per unit volume does it in the opposite direction (see Fig. C-4, Section C, Supporting Information).

The anodes clearly showed a wide distribution of performances (bell-like) depending on their interlaminar spacing. The wide variation of performances had already been noticed from the obtained response surfaces (paraboloid with closed curvature), demonstrating that the optimization process allowed identifying those conditions that led to harness the highest current densities from the electrodes with intermediate interlaminar distance and, consequently, intermediate volumetric surface areas.

In the field of porous anodes for bio-electrochemical applications, conducting structures with increasing area per unit volume are typically pursued, on the premise that the larger the volumetric surface area, the higher the bio-electrochemical performance [16]. In the present study, and in the range of levels evaluated, we demonstrated that the anode performance does not scale directly to the true electrode area (the maximum performance was not obtained from maximum surface-to-volume ratios), revealing that, for the case of the laminated electrodes tested in the presence of urine, a limit to the volumetric surface exists to reach the highest current density. According to the maximum current output for the best-performing anode (E-703), a volume ~ 2.5 times larger than that for the laminanted platform would be needed for the non-porous electrode so as to match the same current levels, which highlights the relevance of the miniaturization of the laminated anode as a way to concentrate a large area in a small volume. In addition, there has to be also highlighted the possibility of performing - with the layered anodes - a flow-through feeding mode (for instance, for the case of recirculation in continuous open/closed-systems), which is clearly not possible for the non-porous counterpart. The findings shown in the **Fig. 3** are in agreement with previous results obtained under model conditions (pure culture of *Geobacter sulurreducens*, not mixed inoculum; with acetate as electron donor, not a complex human urine medium) [25]. In addition, the results of the present study extend those obtained from non-porous graphite anodes for the acclimation of a mixed bacterial culture to increasing concentrations of urine [10], going further this time with the acclimation protocol for its application to porous electrodes, demonstrating that particular urine

concentrations and interlaminar distances are neccesary for getting the optimum bio-electrochemical performance (in accordance to the response surfaces obtained).

As to the best-performing microbial anode (electrode E-703), voltammetry tests as a function of urine concentration were conducted to reveal the evolution of the bio-electrochemical performance with the feeding medium composition (Section F, Supporting Information). The electrical response demonstrated that the microorganisms evolved and remained metabolically active under the experimental conditions used, with processes resembling those for electro-active bacteria confined in porous electrodes fed under flow-through regimes [14,24,25].

3.3. Current densities in the context of urine-fed bio-electrochemical systems

In order to put the maximum current density obtained in this study (electrode E-703: 5.21 $kA.m^{-3}$ or 3.72 $A.m^{-2}$) in context with reported values for other porous anodes used in urine-fed bio-electrochemical systems, areal current densities were compared. It is usually accepted to express and contrast current densities on the basis of the projected anode surface area [17]. However, it has been already pointed out that the use of projected surface areas as a performance indicator should be taken judiciously when comparing porous electrodes, mainly because their complex surface distribution per unit volume is usually far larger than the projected one [18]. In addition, comparisons sometimes exceed what it can be said from a particular system, as the experimental conditions among the different set-ups are usually not exactly the same. Despite all of this, the projected surface area is still the most wiespread performance indicator in bio-electrochemical applications. In this context, we cautiously attemped to frame our results together with those reported for porous anodes in the area of urine-fed bio-electrochemical systems under conditions that - at least - have ensured maximum anode current outputs for non-limited cathode conditions (whenever the case of two-compartment MFCs). Current densities for typical bio-electrochemical systems treating urine by using porous anodes (e.g., carbon veil,

carbon cloth, graphite felt) span around 0.1-0.6 $A.m^{-2}$, on the basis of the projected anode surface area [9,26,28,29,43]. In this frame, the maximum current density recorded in the present study (3.72 $A.m^{-2}$, real anode surface) under the operation conditions used (continuous flow of diluted urine: 10 %v/v) for the top-performance electrode is, at least, promising, particularly thinking of its use in small-scale MFCs.

The miniaturization of MFCs, along with their stacking to reach a compact footprint configuration, has been proposed lately as a convenient strategy to face the main limiting factors of typical MFCs for their practical application at large scale; namely, materials costs, high internal resistances and ohmic losses ocurring when scaling-up the technology [44-46]. In this scenario, the scale-down approach offers advantages associated to the simplicity of the experimental operation, as well as the possibility of getting rid of (or at least reduce) diffusive issues (especially in air-cathode miniaturized MFCs), showing at the same time a competitive advantage by counting on a compact large surface area per anode unit volume. It is precisely at this point that the laminated anodes presented in this study could be exploited at their full potential, especially under a flow-through configuration. This would add large surface areas concentrated in small anode (and tubing) volumes, without experiencing large pressure drops along the feeding circuit. To evaluate these characteristics, the use of the laminated anodes in urine-fed small-scale MFC configurations is currently in progress.

4. Conclusions

Three-dimensional monolithic Ti_4O_7 electrodes with laminar structures were introduced as microbial anodes for urine-fed bio-electrochemical systems. The main conclusions can be summarized as follows:

(i) It is possible to tune the surface area per anode unit volume by controlling the interlaminar distance of the electrode architectures.

(ii) Contrary to typical 3D macroporous anodes with tortuous structures, the laminated configuration allowed profiting from the true surface area when urine feeding was performed as a continuous flow through the anode structures.

(iii) The laminar electrodes represent a valuable option to concentrate large surface areas in a compact configuration for continuous low-pressure drop flowing-through bio-electrochemical applications.

(iv) The optimization of the performance of the microbial anodes *via* the response surface methodology (RSM) allowed saving experimental efforts through an statistical multivariate approach, while simultaneously paved the way to the identification of the levels of the experimental variables that together led to maximizing the volumetric current density.

In this context, the novelty of the present study relies on demonstrating the existence of a trade-off between the accessibility to the internal electrode structure (controlled by the interlaminar distance) and the effective usage of the electrode surface area to optimize the volumetric current density of the laminated microbial anodes, which opens the door to the possibility of modulating on demand the laminated features to impact directly on the output current densities when urine is used as feeding fuel under a flow-through regime.

Declaration of Competing Insterest

The authors declare that they have no known competing financial interests or personal relationships that could have appeared to influence the work reported in this paper.

Acknowledgements

This study was financially supported by the National Research and Council (CONICET, Argentina) and the National Agency for the Promotion of Science and Technology (ANPCyT, Argentina).

Appendix A. Supplementary material

Supplementaty information and R data file to this article can be found online at https (corresponding DOI here).

References

[1] K. Rabaey, L. Angenent, U. Schröder, J. Keller, in Bioelectrochemical systems: from extracelular electron transfer to biotechnological application, IWA Publishing, London, UK, 2010.

[2] B.E. Logan, K. Rabaey, Science 337 (2012) 686-690.

[3] László Koók, Nándor Nemestóthy, Katalin Bélafi-Bakó, PéterBakonyi, Bioelectrochemistry 140 (2021) 107749-107756.

[4] I.A. Ieropoulos, A. Stinchcombe, A.I. Gajda, S. Forbes, I. Merino-Jimenez, G. Pasternak, D. Sanchez-Herranza, J. Greenman, Environ. Sci.: Water Res. Technol. 2 (2016) 336-343.

[5] M.J. Salar-Garcia, O. Obata, H. Kurt, K. Chandran, J. Greenman, I.A. Ieropoulos. Microorganisms 8 (2020) 1921-1936.

[6] C. Santoro, M.J. Salar-Garcia, X.A. Walter, J. You, P. Theodosiou, I. Gajda, O. Obata, J. Winfield, J. Greenman, I.A. Ieropoulos. ChemElectroChem 7(2020) 1312-1331.

[7] X.A. Walter, I. Gajda, S. Forbes, J. Winfield, J. Greenman, I.A. Ieropoulos. Biotechnol Biofuels 9 (2016) 93.

[8] X.A. Walter, S. Forbes, J. Greenman, I.A. Ieropoulos. Sustain. Energy Technol. Assess. 14 (2016) 74-79.

[9] S.G. Barbosa, L. Peixoto, A. Ter Heijne, P. Kuntke, M.M. Alves, M.A. Pereira, Environ. Sci.: Water Res. Technol. 3 (2017) 897-904.

[10] M. Prudente, D.A. Massazza, J.P. Busalmen, H.E. Romeo. Bioelectrochemistry 137 (2021) 107639-107646.

[11] R-B. Song, Y. Wu, Z-Q. Lin, J. Xie, C.H. Tan, J.S.C. Loo, B. Cao, J-R. Zhang, J-J. Zhu, Q. Zhang. Angew. Chem. 129 (2017) 10516-10520.

[12] C. Picioreanu, M.C.M. van Loosdrecht, J.J. Heijnen. Biotechnol. Bioeng. 69 (2000) 504-515.

[13] V. Flexer, J. Chen, B.C. Donose, P. Sherrell, G.G. Wallace, J. Keller. Energy Environ. Sci. 6 (2013) 1291-1298.

[14] D.A. Massazza, R. Parra, J.P. Busalmen, H.E. Romeo. Energy Environ. Sci. 8 (2015) 2707-2712.

[15] A. Baudler, M. Langner, C. Rohr, A. Greiner, U. Schröder. ChemSusChem 10 (2017) 253-257.

[16] X. Xie, C. Criddle, Y. Cui. Energy Environ. Sci. 8 (2015) 3418-3441.

[17] P. Chong, B. Erable, A. Bergel. Bioresour. Technol. 289 (2019) 121641-121652.

[18] M. Sharma, S. Bajracharya, S. Gildemyn, S.A. Patil, Y. Alvarez-Gallego, D. Pant, K. Rabaey, X. Dominguez-Benetton. Electrochim. Acta 140 (2014) 191-208.

[19] L. Robuschi, J.P. Tomba, G.D. Schrott, P.S. Bonanni, P.M. Desimone, J.P. Busalmen. Angew. Chem. Int. Ed. 52 (2013) 925-928.

[20] G.D. Schrott, M.V. Ordoñez, L. Robuschi, J.P. Busalmen. ChemSusChem 7 (2014) 598-603.

[21] G. Reguera, K.P. Nevin, J.S. Nicoll, S.F. Covalla, T.L. Woodard, D.R. Lovley. Appl. Environ. Microbiol. 72 (2006) 7345-7348.

[22] S. Ishii, K. Watanabe, S. Yabuki, B.E. Logan, Y. Sekiguchi. Appl. Environ. Microbiol 74 (2008) 7348-7355.

[23] K.P. Nevin, H. Richter, S.F. Covalla, J.P. Johnson, T.L. Woodard, A.L. Orloff, H. Jia, M. Zhang, D.R. Lovley. Environ. Microbiol. 10 (2008) 2505-2514.

[24] K. Katuri, M.L. Ferrer, M.C. Gutiérrez, R. Jiménez, F. del Monte, D. Leech. Energy Environ. Sci. 4 (2011) 4201-4210.

[25] D. Massazza, J.P. Busalmen, R. Parra, H.E. Romeo. J. Mater. Chem. A 6 (2018) 10019-10027.

[26] I.A. Ieropoulos, J. Greenman, C. Melhuish. Phys. Chem. Chem. Phys. 14 (2012) 94-98.

[27] I.A. Ieropoulos, P. Ledezma, A. Stinchcombe, G. Papaharalabos, C. Melhuish, J. Greenman. Phys. Chem. Chem. Phys. 15 (2013) 15312-15316.

[28] C. Santoro, I.A. Ieropoulos, J. Greenman, P. Cristiani, T. Vadas, A. Mackay, B. Li. J. Power Sour. 238 (2013) 190-196.

[29] D.D. Shreeram, D.J. Hassett, D.W. Schaefer. J. Ind. Microbiol. Biotechnol. 43 (2016) 103-107.

[30] Y. Zhou, L. Tang, Z. Liu, J. Hou, W. Chen, Y. Li, L. Sang. Biochem. Eng. J. 124 (2017) 36-43.

[31] A. Kitada, G. Hasegawa, Y. Kobayashi, K. Kanamori, K. Nakanishi and H. Kageyama, J. Am. Chem. Soc. 134 (2012) 10894-10898.

[32] G. Boeije, R. Corstanje, A. Rottiers, D. Schowanek, Chemosphere 38 (1999) 699-709.

[33] M. Rimboud, D. Pocaznoi, B. Erable, A. Bergel. Phys.Chem.Chem.Phys. 16 (2014) 16349.

[34] C.I. Torres, A. Kato Marcus, B.E. Rittmann. Biotechnol. Bioeng. 100 (2008) 872-881.

[35] K. Kolbrecka, J. Przyluski. Electrochim. Acta 39 (1994) 1591-1595.

[36] M.F.S. Barni, L.I. Doumic, R.A. Procaccini, M.A. Ayude, H.E. Romeo. J. Environ. Manage. 263 (2020) 110403.

[37] ZView 3.4e©, Scribner Associates, Inc.

[38] ZSimpWin 3.21© EChem Software.

[39] R. Leardi. Anal. Chim. Acta 652 (2009) 161-172.

[40] A.I. Khuri, S. Mukhopadhyay. WIREs Computational Statistics 2 (2010) 127-257.

[41] M.A. Bezerra, R.E. Santelli, E.P. Oliveira, L.S. Villar, L.A. Escaleira. Talanta 76 (2008) 965-977.

[42] R.V. Lenth. J. Stat. Softw. 32 (2009) 1-17.

[43] S.G. Barbosa, T. Rodrigues, L. Peixoto, P. Kuntke, M.M. Alves, M.A. Pereira, A. Ter Heijne. Renew. Energ. 139 (2019) 936-943.

[44] I.A. Ieropoulos, J. Greenman, C. Melhuish. Bioelectrochemistry 78 (2010) 44-50.

[45] J. Chouler, G.A. Padgett, P.J. Cameron, K. Preuss, M.M. Titirici, I.A. Ieropoulos, M. Di Lorenzo. Electrochim. Acta 192 (2016) 89-98.

[46] I.A. Ieropoulos, J. Greenman, C. Melhuish. Int. J. Hydrog. Energy 38 (2013) 492-496.

Declaration of interests

☒ The authors declare that they have no known competing financial interests or personal relationships that could have appeared to influence the work reported in this paper.

☐ The authors declare the following financial interests/personal relationships which may be considered as potential competing interests:

Highlights

- Laminated Ti_4O_7 microbial anodes were used to produce current from human urine.
- Anode volumetric current densities were tuned by modifying the interlaminar distance.
- The response surface methodology (RSM) was used to optimize the anode performance.
- Maximum current densities of 5.2 kA.m-3 were obtained from the optimized conditions.